

Control of corolla monosymmetry in the Brassicaceae *Iberis amara*

Andrea Busch* and Sabine Zachgo*^{††}

*Max Planck Institute for Plant Breeding Research, Carl-von-Linné Weg 10, 50829 Köln, Germany; and [†]Department of Botany, University of Osnabrück, Barbarastrasse 11, 49076 Osnabrück, Germany

Edited by Enrico Coen, John Innes Centre, Norwich, United Kingdom, and approved August 28, 2007 (received for review June 11, 2007)

Establishment of morphological novelties has contributed to the enormous diversification of floral architecture. One such novelty, flower monosymmetry, is assumed to have evolved several times independently during angiosperm evolution. To date, analysis of monosymmetry regulation has focused on species from taxa where monosymmetry prevails, such as the Lamiales and Fabaceae. In *Antirrhinum majus*, formation of a monosymmetric corolla is specified by the activity of the TCP transcription factors *CYCLOIDEA* (*CYC*) and *DICHOTOMA* (*DICH*). It was shown that establishment of monosymmetry likely requires an early asymmetric floral expression of *CYC* homologs that needs to be maintained until late floral stages. To understand how *CYC* homologs might have been recruited during evolution to establish monosymmetry, we characterized the likely *CYC* ortholog *laTCP1* from *Iberis amara* (Brassicaceae). Species of the genus *Iberis* form a monosymmetric corolla, whereas the Brassicaceae are otherwise dominated by genera developing a polysymmetric corolla. Instead of four equally sized petals, *I. amara* produces two small adaxial and two large abaxial petals. The timing of *laTCP1* expression differs from that of its *Arabidopsis* homolog *TCPI* and other *CYC* homologs. *laTCP1* lacks an asymmetric early expression but displays a very strong differential expression in the corolla at later floral stages, when the strongest unequal petal growth occurs. Analysis of occasionally occurring *peloric Iberis* flower variants and comparative functional studies of TCP homologs in *Arabidopsis* demonstrate the importance of an altered temporal *laTCP1* expression within the Brassicaceae to govern the formation of a monosymmetric corolla.

floral symmetry | *laTCP1*

The generation of morphological novelties has contributed to the diversification of angiosperm flowers. Particularly in the corolla, which protects inner male and female organs and exerts an important function in pollinator attraction, modifications affecting color, size, shape, scent production, and symmetry have generated a remarkable diversity. Approximately 130–90 million years ago, in the early Cretaceous, flower structures were simple, and all organs in one whorl resembled each other (1, 2), as can still be observed in some extant basal eudicots, for instance in the Papaveraceae. These flowers are polysymmetric (or radially symmetric) with several planes of symmetry dividing the flower. First traces of monosymmetric (or zygomorphic) flowers, with one single symmetry plane along the dorsoventral axis, occurred in fossil records from the late Cretaceous, dating back ≈70 million years (3). Coevolution with pollinators, such as insects, led to the establishment of specialized floral morphologies that possibly contributed to speciation. Some of the species-richest angiosperm taxa, like the Lamiales, Leguminosae, and Orchidaceae, are dominated by monosymmetric flowers that often guide pollinators to access flowers from a particular direction (4–7). These flowers produce ad- and abaxial petals of different shapes and often, as in *Antirrhinum*, abaxial petals form specialized landing platforms for pollinators. Because several monosymmetric clades are nested within polysymmetric clades, it is assumed that floral monosymmetry evolved several times independently from the ancestral polysymmetric condition (8, 9).

Evolution of novel traits, such as floral monosymmetry, is driven by genetic changes. Comprehensive knowledge of the molecular mechanisms controlling formation of a monosymmetric corolla has been gained by analysis of loss-of-function mutants, particularly from the model species *Antirrhinum majus*. This process is controlled by two central regulatory genes with partially redundant functions, the TCP transcription factors *CYCLOIDEA* (*CYC*) and *DICHOTOMA* (*DICH*) (10, 11). In *cyc dich* double mutants, monosymmetry is lost and instead, flowers with a polysymmetric corolla are formed that are composed solely of abaxial petals (10). In single *cyc* or *dich* mutants, flowers are only weakly abaxialized, indicating that a partial subfunctionalization of the two recently evolved paralogs has occurred after duplication of the ancestral gene (11–13). A duplication event has also been reported for species from the Fabaceae (14, 15), but not for the Brassicaceae. The model species *Arabidopsis thaliana* harbors only one copy of the *CYC* ortholog, namely *TCPI*. In *A. majus*, *CYC* and *DICH* are expressed in the adaxial domain of the young flower meristem, and asymmetric *CYC* expression is maintained until late floral stages. Late *DICH* expression is restricted to the inner domain of adaxial petal lobes, reflecting its function in regulating internal petal symmetry (11). The MYB-like transcription factors *RADIALIS* (*RAD*; ref. 16) and *DIVARICATA* (*DIV*; refs. 17 and 18) participate in symmetry regulation. *RAD* is a target gene of *CYC* (19), and *rad* mutants, similar to *cyc* mutants, form partially abaxialized flowers (10). *RAD* acts antagonistically to *DIV* (16), a factor promoting abaxial petal identity.

TCP transcription factors form a diverse family. All members possess a conserved TCP domain that is unique to plants and adopts a helix–loop–helix structure (20). The closely related TCP genes *CYC*, *TCPI*, and *TEOSINTE BRANCHED 1* (*TB1*) from *Zea mays* (21) cluster together in the so-called ECE clade (22) and share an arginine-rich R domain (20). The function of *TCPI* from *Arabidopsis*, a species with a polysymmetric corolla, remains to be shown, because mutants do not exhibit obvious phenotypes (23). *TCPI* is only transiently expressed in the adaxial domain of the young floral meristem, which might not be sufficient to regulate monosymmetry in the second whorl (24). This observation supports the assumption that the ancestral progenitor of the *CYC/TCPI* gene was asymmetrically expressed even though the presumed ancestral corolla state was polysymmetric (19, 24). So far, analysis of *CYC* homologs focused on species from taxa forming monosymmetric corollae, such as *Linaria*, *Mohavea*, and *Lotus*. The *CYC/TCPI* homologs of these

Author contributions: S.Z. designed research; A.B. performed research; A.B. contributed new reagents/analytic tools; A.B. and S.Z. analyzed data; and A.B. and S.Z. wrote the paper.

The authors declare no conflict of interest.

This article is a PNAS Direct Submission.

Data deposition: The sequences reported in this paper have been deposited in the GenBank database [accession nos. *laRAN3* (EU145777), *laH4* (EU145778), and *laTCP1* (EU145779)].

^{††}To whom correspondence should be addressed. E-mail: szachgo@mpiz-koeln.mpg.de.

This article contains supporting information online at www.pnas.org/cgi/content/full/0705338104/DC1.

© 2007 by The National Academy of Sciences of the USA

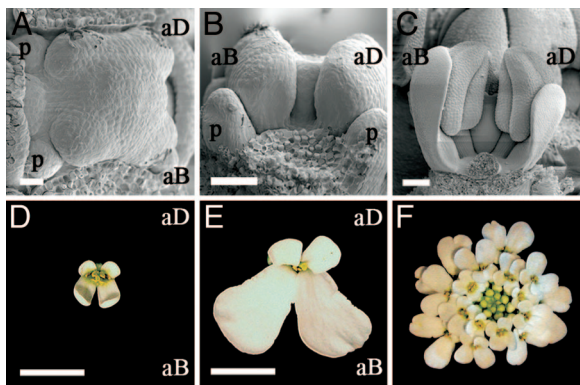


Fig. 1. Development of the monosymmetric corolla in *I. amara*. Different stages of *Iberis* flower development are shown. (A–C) Developmental stages before anthesis were monitored under the SEM; sepals were removed to reveal inner organs. (A) After simultaneous initiation, adaxial (aD) and abaxial (aB) petal (p) primordia are of equal size. Central stamen primordia arise slightly before the lateral stamen primordia, developing between the adaxial and abaxial petals. The gynoecium appears as a central dome. (B) At the onset of stamen differentiation, when filament and anther become distinguishable, adaxial and abaxial petals start to differ in size, with the abaxial petals being slightly larger. (C) Petal size difference slowly increases until anthesis of the flower. A lateral stamen is removed in B and C. (D) After flower opening, the petal size difference strongly increases from the young stage A1 to the fully mature stage A2 (E). (F) The young inflorescence of *Iberis* shows a corymboid architecture that gives it the appearance of one single, large flower. (Scale bars: A–C, 50 μm ; D and E, 5 mm.)

species all exhibit an asymmetric expression during early and later floral development, similar to *A. majus* (12, 14, 25). For those species, where loss-of-function or transgenic knockdown mutants were analyzed, data support a role for the investigated *TCP* genes in floral symmetry formation (10, 14, 25).

Here, we report an approach to elucidate the molecular mechanism that led to the establishment of monosymmetry in the Brassicaceae. The Brassicaceae comprise ≈ 350 genera (26) whose members mainly form polysymmetric corollae. However, flowers of three genera, *Iberis*, *Teesdalia*, and *Calepina*, develop a monosymmetric corolla with differentially sized petal pairs. *Iberis* species exhibit the strongest size differences between the small adaxial and large abaxial petals. We isolated the *CYC/TCP1* ortholog of *Iberis amara*, *IaTCP1*, and investigated its function during flower development. Studying a nonmodel species from the Brassicaceae allowed us to conduct functional analyses in *Arabidopsis*. Together with expression studies and analysis of a rare natural *peloric Iberis* flower variant, our data indicate that changes in the timing of the expression of the orthologous *TCP1* gene *IaTCP1* control the formation of a monosymmetric corolla in the Brassicaceae.

Results

Development of the Monosymmetric *I. amara* Corolla. To unravel the molecular mechanism controlling corolla monosymmetry for-

mation in *I. amara*, we first characterized the dynamics of unequal ad- and abaxial petal morphogenesis. Flower development starts with initiation of sepal primordia, with the abaxial sepal arising first and finally being slightly larger than the other sepals, similar to what has been described for *A. thaliana* (27). Initially, the four *I. amara* petal primordia are formed simultaneously as equally sized protrusions in ad- and abaxial positions on the floral meristem (Fig. 1A). Deviations in petal growth start to become apparent at the onset of stamen differentiation (Fig. 1B). From then on, the size difference between the two petal pairs increases continuously throughout flower development (Fig. 1C), generating abaxial petals that are 1.6 times larger than adaxial petals at anthesis, when the flower opens (stage A1; Fig. 1D and Table 1). Unequal petal growth is strongly enhanced after anthesis until flowers reach maturity (stage A2; compare Fig. 1D and E). Thereby, the petal size ratio is increased from 1.6- up to 3.7-fold (Table 1).

To determine whether this unequal petal growth is due to an altered rate of cell proliferation and/or cell expansion, sizes of adaxial epidermal petal cells were quantified and compared. Cell sizes of ad- and abaxial petals are similar in flowers of stages A1 and A2, ≈ 240 and $510 \mu\text{m}^2$, respectively (Table 1). Given that observation, it is likely that unequal cell proliferation rather than differential cell expansion accounts for the strong petal size differences and thus for the formation of the monosymmetric corolla in *I. amara*.

Iberis corolla monosymmetry allows flowers to sit closely together without canoping neighboring flowers with protruding adaxial petals. Along with retarded early internode elongation and pedicel growth, this contributes to shaping the peculiar architecture of young *I. amara* inflorescences. Inflorescences adopt a corymboid structure with a flattened top and superficially resemble one single flower (Fig. 1F), an effect typically generated by the umbel of Apiaceae.

Isolation and Expression Analysis of *IaTCP1*. To test whether a *CYC/TCP1* homolog is involved in controlling the formation of unequally sized *Iberis* petal pairs, we isolated *IaTCP1* from *I. amara*. The 1,480-nt-long *IaTCP1* transcript contains an ORF of 981 nt coding for a predicted *IaTCP1* protein of 327 aa. As characteristic for *CYC/TCP1* homologs, *IaTCP1* contains a *TCP* domain of 59 aa that adopts a basic helix–loop–helix structure known to be involved in DNA binding and protein dimerization (28). Also, an R domain is present, likely forming a coiled-coil structure that might function in protein–protein interactions (20, 29). *IaTCP1* and *TCP1*, the likely *CYC* ortholog from *Arabidopsis* (23), share 64% identity at the nucleotide and 59% identity at the protein level. Considering only the *TCP* domain, amino acid identity increases up to 95%, which together with phylogenetic tree analysis [supporting information (SI) Fig. 6] supports the assumption that *IaTCP1* represents the orthologous *TCP1* gene.

IaTCP1 expression levels were quantified by RT-PCR experiments in vegetative and floral *Iberis* organs (Fig. 2). *IaTCP1* expression is low in leaves and shoots, as well as in inflorescences, flowers before anthesis, fully mature flowers, and gynoecia.

Table 1. Quantification of *I. amara* petal surface area and petal cell size

	Petal area, mm^2		Petal cell size, μm^2	
	St. A1	St. A2	St. A1	St. A2
aD petals	3.6 ± 0.8	10.2 ± 2.1	241.92 ± 60.04	490.91 ± 94.94
aB petals	5.7 ± 1.5	38.1 ± 8.0	239.66 ± 49.57	534.40 ± 87.94
aB/aD	1.6 ± 0.2	3.7 ± 0.4	0.99 ± 0.32	1.09 ± 0.27

Values with standard deviation are given for average adaxial (aD) and abaxial (aB) petal surface area (mm^2) and cell size (μm^2) from flowers at stages (St.) A1 and A2. Differences between adaxial and abaxial petal values are given as ratios (aB/aD).

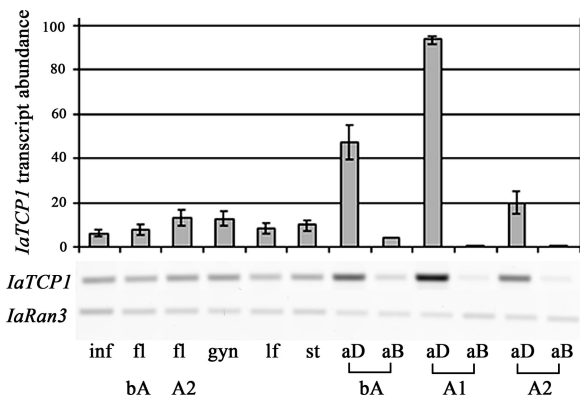


Fig. 2. RT-PCR analysis of *IaTCP1* expression in vegetative and floral organs. (Upper) The graph depicts average *IaTCP1* transcript values from three independent reactions, normalized to the expression strength of *IaRan3*. Error bars indicate standard deviations. *IaTCP1* is weakly expressed in leaves (lf) and shoots (st), as well as in inflorescences (inf), flowers before anthesis (fl bA), mature flowers (fl A2), and gynoecia (gyn). A dynamic differential expression becomes apparent in separately analyzed adaxial (aD) and abaxial (aB) petals isolated from flowers before anthesis (bA), from young flowers after anthesis (A1), and from fully mature flowers (A2). Expression is always stronger in adaxial than in abaxial petals. (Lower) Gel image of a representative *IaTCP1* and *IaRan3* RT-PCR.

However, when ad- and abaxial petal pairs were separately analyzed, a strong differential *IaTCP1* expression was detected. Expression is high in the two smaller adaxial petals and weaker in the large abaxial petals. This differential *IaTCP1* expression is dynamic throughout corolla development. Before anthesis, *IaTCP1* expression is ≈ 10 -fold (10.96 ± 1.31) higher in adaxial as compared with abaxial petals. The difference increases up to a peak of >90 -fold (93.18 ± 2.21) just after anthesis when buds open and decreases to a level of almost 20-fold (19.17 ± 4.56), once flowers reach maturity.

In situ hybridization experiments were carried out to determine the tissue-specific *IaTCP1* expression at earlier floral stages (Fig. 3). For the *Arabidopsis TCP1* gene, early and transient asymmetric expression in the young floral meristem has been detected, which vanishes before floral organ primordia are initiated (24). No distinct asymmetric *IaTCP1* expression could be detected in young floral *Iberis* meristems (Fig. 3A). After onset of stamen differentiation, low *IaTCP1* expression was observed in young petals and stamens (Fig. 3B). However, once floral organ differentiation advanced further, a stronger *IaTCP1* expression was detectable in adaxial compared with abaxial petals (Fig. 3C). Therefore, in contrast to the expression of the orthologous *Arabidopsis TCP1* gene, asymmetric *IaTCP1* expression is established during later flower development, after floral primordia are initiated and organs started to differentiate.

Because the observed petal size difference is likely caused by a differential rate of cell proliferation, *Histone 4*, a cell cycle marker gene indicative of the S phase (30), was isolated from *Iberis* (*IaH4*) and its expression analyzed. Generally, *IaH4* is strongly expressed in regions with high cell proliferation activity, e.g., in inflorescence and floral meristems (data not shown). Comparing serial sections probed with *IaTCP1* and *IaH4*, we detected a complementary RNA expression strength in young petals. *IaTCP1* is expressed more strongly in adaxial petals (Fig. 3C), whereas *IaH4* transcript is present in a larger number of abaxial compared with adaxial petal cells (Fig. 3D). This implies that unequal petal sizes are established by different cell proliferation rates in the two petal pairs. The dynamic of *IaTCP1* expression correlates with the dynamic of petal morphogenesis. This observation supports a function for *IaTCP1* during late

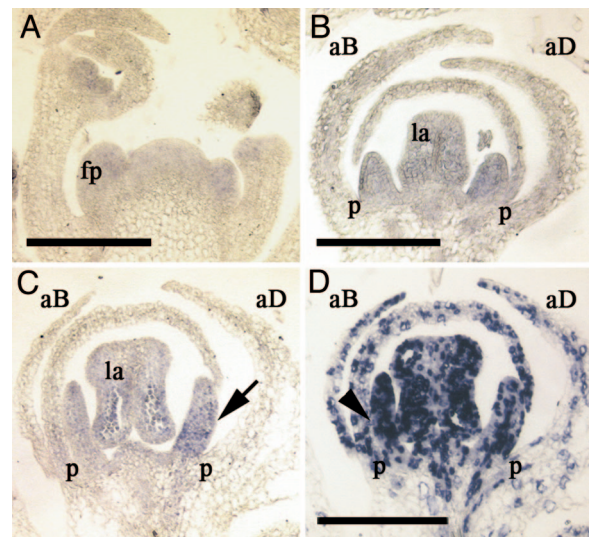


Fig. 3. *In situ* expression pattern of *IaTCP1* and *IaH4* in young *Iberis* flowers. (A–C) *IaTCP1* antisense probe hybridized to a longitudinal section through the *Iberis* inflorescence meristem and young developing flowers. (A) No distinct asymmetric *IaTCP1* expression is detectable in the inflorescence meristem and adjacent young floral primordia (fp). (B) After onset of stamen differentiation, weak *IaTCP1* expression becomes visible in petals (p) where similar expression levels were detected in adaxial (aD) and abaxial (aB) petals. Expression was also observed in anthers (lateral anther, la). (C) An asymmetric *IaTCP1* expression becomes apparent in later floral stages, where a stronger signal was detectable in adaxial (aD) than in abaxial (aB) petals. (D) Antisense *IaH4* probe was hybridized to serial sections shown in C revealing that more cells express *IaH4* in abaxial petals (arrowhead) compared with adaxial ones, which indicates higher cell proliferation activity in abaxial petals. (Scale bars: 200 μm .)

petal development, reaching its maximal activity probably around the time of anthesis.

Analysis of a Peloric Flower Variant of *I. amara*. During cultivation of a large number of *I. amara* plants, we could identify a few plants that randomly produced one to two flowers in an inflorescence where corolla monosymmetry was lost. These flower variants showed an abaxialized corolla, where the two small adaxial petals of wild-type *Iberis* flowers (Fig. 4A) were replaced by two large abaxialized petals (Fig. 4B). Sufficient petal material from these *peloric* flower variants could be harvested from stage A2 to compare the *IaTCP1* expression levels in wild-type and *peloric* petals by RT-PCR. Wild-type petals showed a strong *IaTCP1* expression (Fig. 4C). Given the above-reported wild-type RT-PCR data, this is likely due to high *IaTCP1* expression in adaxial petals. However, in petals from the *peloric* variant, the

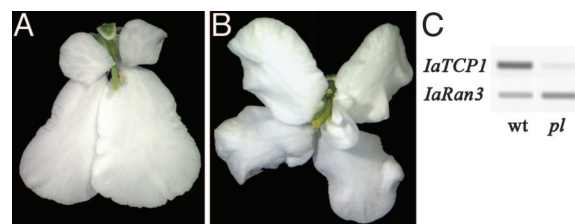


Fig. 4. A *peloric* flower variant of *I. amara* develops an abaxialized corolla. (A) Wild-type flower at stage A2. (B) Naturally occurring *peloric* flower variant with only abaxialized petals. (C) Representative RT-PCR result showing reduced *IaTCP1* expression in *peloric* (pl) compared with wild-type (wt) corollae. Quantification of four RT-PCRs revealed that >27 -fold (27.64 ± 9.81) more *IaTCP1* transcript was detectable in wild-type petals compared with *peloric* petals. For normalization, *IaRan3* expression level was determined.

occurs late in flower development, after anthesis. Comparison of cell sizes from ad- and abaxial petals revealed similar values, indicating that the unequal petal size is due to changes in cell proliferation rather than cell expansion.

Elevated transcript levels in adaxial petals compared with abaxial ones became recognizable by *in situ* hybridization experiments after stamens started to differentiate. RT-PCR revealed a dynamic differential *IaTCP1* expression, with a maximal expression difference occurring after anthesis when the strongest gain in unequal petal growth is realized. Expression analysis using the cell cycle marker *IaH4* further corroborates the assumption that differential petal growth is realized by unequal cell proliferation, because *IaH4* and *IaTCP1* expression strength differences in ad- and abaxial petal pairs are complementary. Late and enhanced *IaTCP1* expression in adaxial petals might expose a negative effect on cell proliferation leading to the development of smaller adaxial petals compared with abaxial ones and thereby to a monosymmetric corolla. A negative effect on cell cycle progression has also been described for other *TCP* transcription factors, such as *CYC* and *CINCINNATA* from *Antirrhinum* and *TCP2* and *TCP4* from *Arabidopsis* (30–32).

The timing of *IaTCP1* mRNA expression differs from that described for other *CYC/TCP1* homologs from species with a monosymmetric corolla belonging to the Asterids (*Antirrhinum* and *Linaria*; refs. 10 and 25) or Rosid clades, other than the Brassicaceae (*Lotus* and *Lupinus*; refs. 14 and 33). There, respective *CYC* homologs are expressed in the adaxial domain of the developing flower, starting at early floral meristem stages and being maintained until late floral stages. In *Arabidopsis*, developing a polysymmetric corolla, *TCP1* is also expressed early in the adaxial region of the floral meristem. However, this expression is transient and disappears before floral organ primordia are initiated, which might account for the lack of monosymmetry in the corolla (24). As an early asymmetry of *CYC/TCP1* gene expression is common to both Asterids and Rosids, it is assumed that it might represent the ancient expression state in the common ancestor (19, 24). Accordingly, early asymmetric *IaTCP1* expression might have been lost in *Iberis*. Alternatively, instead of a common ancestral expression pattern, a high flexibility in modulating *CYC/TCP1* gene expression could have established an early and/or late asymmetric expression independently several times. Further expression studies with *CYC/TCP1* homologs from evolutionary informative monosymmetric as well as polysymmetric species will help to elucidate this question. Development of a more complex monosymmetric corolla, such as that of *A. majus*, depends on petal form and folding in addition to petal size differences and might require an earlier onset and maintenance of *CYC* expression. Corolla monosymmetry in *Iberis* is revealed only by different petal pair sizes and, because it is a less complex feature, it bears the potential to unravel first, initial changes in regulatory networks that generated monosymmetry in the Brassicaceae. Establishment of the late *IaTCP1* expression in *Iberis*, along with high expression differences in the two petal pairs, seems to govern the formation of unequal ad- and abaxial petals in *Iberis*.

Function of *IaTCP1* and *TCP1*, but Not *CYC*, Is Conserved in the Brassicaceae. In rarely occurring *peloric Iberis* flowers, where all four petals adopt the size of abaxial petals, *IaTCP1* expression was strongly reduced, further supporting a function of *IaTCP1* in shaping a monosymmetric corolla. *Peloric* flowers with abaxialized petals have been described for other monosymmetric species. In *Antirrhinum*, *peloric* flower formation is caused by transposon insertions in the *CYC* and *DICH* loci, disrupting their function (10, 11). In *peloric Linaria* flowers, the respective *CYC* ortholog is silenced by hypermethylation (25). *IaTCP1* expression, however, is not completely abolished in *peloric Iberis* petals,

but the remaining transcript level is likely below the threshold required to exert a negative effect on petal growth.

Additional functional data were obtained by overexpression of *IaTCP1* in the related cruciferous species *A. thaliana*. Transgenic plants with an intermediate phenotype produce flowers with an approximately two times reduced petal size compared with wild-type flowers. Similar to the results from cell size measurement in *Iberis* petals, reduction of the petal area in *Arabidopsis* plants overexpressing *IaTCP1* is likely achieved via affecting cell proliferation rates rather than the extend of cell expansion. Overexpression of the orthologous *Arabidopsis TCP1* gene causes the same phenotypes. Thus, both *TCP* proteins show similar effects upon ectopic expression, indicating that their cis- and transregulatory functions, involved in cell cycle regulation, are conserved. This observation leads to the assumption that establishment of the monosymmetric corolla in *Iberis* is largely accounted for by strong and asymmetric *IaTCP1* expression during late petal development, whereas the early transient floral *TCP1* expression in *Arabidopsis* might not be sufficient to affect morphogenesis. Contrarily, ectopic expression of *CYC* from *Antirrhinum*, belonging to the Asterid clade, leads to the formation of *Arabidopsis* flowers with enlarged petals. Similar results were recently obtained by Costa *et al.* (19), who used an inducible *CYC* expression system that caused enhanced growth of *Arabidopsis* petals. However, this size increase was mainly achieved by enhanced cell expansion. The authors demonstrated that *CYC* activity in transgenic *Arabidopsis* flowers is not able to activate endogenous *Arabidopsis RAD* genes, whereas the *Antirrhinum RAD* gene is a direct *CYC* target (19). Therefore, *TCP* genes from Rosids and Asterids seem to have diverged strongly at the level of protein function since they separated from their last common ancestor. This divergence, along with expression differences, might have led to a specific interplay between cis- and transregulatory mechanisms in the different taxa. Amino acid comparison of *TCP* domains shows that a neutral alanine found in *TCP1* (20) and in *IaTCP1* is replaced by a hydrophobic proline in *CYC*. Secondary structure predictions (ref. 20; data not shown) indicate this might have an impact on the shape of the basic helix–loop–helix structure which could account for differences in protein–protein interactions and/or DNA binding. Subfunctionalization of duplicated *TCP* genes likely also contributed to more complex flower morphologies as described for *Antirrhinum* and *Mohavea* (11, 12). However, in *Iberis*, no other close *IaTCP1* homolog could be isolated, indicating that, as in *Arabidopsis*, no duplication event occurred.

What could be the adaptive advantage of corolla monosymmetry in a cruciferous species? Monosymmetry is considered a key innovation that contributed greatly to the successful radiation of angiosperm taxa like the Lamiales, Leguminosae, and Orchidaceae (5). The advantage generally accredited to monosymmetry is an enhanced precision of pollination via guidance of the approaching insects and a facilitated recognition by pollinators (6, 34). For the cruciferous species *Erysimum mediohispanicum*, it has been shown that the number of pollinator visits is increased for individuals forming monosymmetrical flowers (35). Our data show that altered timing of *IaTCP1* expression governs unequal petal growth, allowing flowers to sit closely together within young inflorescences. This, along with retarded internode and pedicel elongation, shapes an untypical cruciferous inflorescence that adopts a corymboid architecture superficially resembling one large single flower. It will be intriguing to determine the effect of the combined morphological changes in *Iberis* on pollinator attraction.

To conclude, the altered temporal expression of a key regulator is a mechanism to generate morphological differences in closely related species from one family. This can serve as a basis to unravel how more complex morphological changes might have evolved between distantly related species by evolutionary tinkering.

Materials and Methods

Plant Material and Growth Conditions. *I. amara* seeds were obtained from Saatgut Kiepenkerl (Everswinkel, Germany). Plants were grown in the greenhouse or in a field at the Max Planck Institute for Plant Breeding Research (Cologne, Germany). Transgenic and wild-type *A. thaliana* (Col.) plants were grown at 20°C with 13-h light/11-h dark cycles.

Morphological Analyses. For scanning electronic microscopy, material was either prepared after critical-point drying (36) or frozen in liquid nitrogen. Material was sputter-coated with gold and examined with a digital scanning microscope (DSM940; Zeiss, Oberkochen, Germany). To determine the petal surface area, pictures were taken with a binocular (MZELIII; Leica, Wetzlar, Germany). Quantification of petal surface area and cell size was performed by using IMAGEJ 1.32J (<http://rsb.info.nih.gov/nih-image>). Averages of petal surface area were determined by measurement of at least 27 petals for each petal type/phenotypic category. For recording adaxial epidermal petal cell sizes, the upper third of at least seven petals was analyzed, and values were calculated based on a minimum of 200 measured cells. Young flowers just after flower opening (anthesis) were defined as stage A1 flowers (Fig. 1D). Fully mature flowers, releasing pollen, were determined as stage A2 flowers (Fig. 1E). For morphological and molecular analysis of *I. amara* stage A1 and A2 petals, flowers were isolated from inflorescences possessing up to 20 open flowers, such as shown in Fig. 1F.

Isolation of Nucleic Acids and Expression Analysis. Total RNA was isolated with the RNeasy Plant Mini kit (Qiagen, Valencia, CA). *IaTCP1* was isolated from genomic *Iberis* DNA by using *A. thaliana* *TCPI*-specific primers (for primer sequences, see *SI Data*). Remaining sequence and transcript length information was obtained conducting 3' RACE (FirstChoice RLM-Race; Ambion, Austin, TX) and 5' RACE (5'/3' RACE Kit; Roche, Indianapolis, IN) experiments. Sequences were cloned into the pCR2.1 (Invitrogen, Carlsbad, CA) and pGEM-T Easy (Promega, Madison, WI) vectors. RT-PCR analysis was performed as described (37) by using 1.8 µg of total RNA for cDNA synthesis. PCRs were carried out at an annealing temperature of 60°C, followed by 24 cycles for *I. amara* and 19 cycles for transgenic *Arabidopsis* plants. Averages of *IaTCP1* expression in *I. amara* corollae are based on three PCR repetitions. Transcript abun-

dance was quantified by using ImageQuant 5.2 (Molecular Dynamics, Sunnyvale, CA). For normalization, the *I. amara* homolog of the *A. thaliana* *Ran3 GTPase* (At5g55190) was isolated (*IaRan3*) and amplified with 23 cycles. Sequence comparison was carried out by using the program DNAMAN 4.0 (Lynnon BioSoft, Los Angeles, CA).

In Situ Hybridization. A 1,386-bp-long *IaTCP1* fragment spanning the TCP and R domain was cloned into the vector pCR2.1 and used as a template for RNA probe preparation after vector linearization with HindIII. A 274-bp-long *I. amara* *Histone 4 (IaH4)* DNA fragment was isolated by using primers specific for *H4* from *A. thaliana* (At5g59690) and cloned into the pGEM-T Easy vector. A reverse primer containing the T7-binding domain was used to prepare a PCR template for transcription. Digoxigenin-labeled riboprobes of *IaTCP1* and *IaH4* were made by using DIG RNA labeling mix and T7 Polymerase (Roche), and hybridizations were carried out as described by Zachgo (38).

Transgenic Plants. Complete coding sequences of *IaTCP1*, *TCPI*, and *CYC* were isolated from *I. amara*, *A. thaliana*, and *A. majus*, respectively. DNA fragments were cloned into pGEM-T Easy, sequenced, and subcloned into pBAR35S (AJ251014), carrying a CaMV35S promoter/terminator cassette. Constructs were introduced into *A. thaliana* plants by floral dip (39) by using the *Agrobacterium tumefaciens* strain GV3101. Transgenic plants were selected by spraying with 0.1% vol/vol BASTA (AgrEvo, Düsseldorf, Germany). Heritability of morphological changes observed in T1 populations was confirmed by analyzing T2 plants. To correlate phenotype strength of transgenic plants with *IaTCP1* transcript abundance, RT-PCRs were conducted with inflorescences from 10 intermediate and 10 strong phenotype T2 plants, respectively. T2 plants were generated by selfing the intermediate T1 plant 35S::*IaTCP1*/2. For normalization, *A. thaliana* *Ran3 GTPase* (At5g55190) was amplified with 21 cycles.

We thank Zsuzsanna Schwarz-Sommer, Heinz Saedler, and Johanna Schmitt for comments on the manuscript. S.Z. is grateful to Heinz Saedler for ongoing support and stimulating discussions. A.B. received a scholarship from the German founding agency Deutsche Forschungsgemeinschaft (DFG; Graduierten Kolleg, "Molecular analysis of developmental processes"). This work was supported by DFG Grant Za 259/6-1 (to S.Z.).

- Crane PR, Friis EM, Pedersen KR (1995) *Nature* 374:27–33.
- Friis EM, Pedersen KR, Crane PR (2001) *Nature* 410:357–360.
- Crepet WL (1996) *Rev Palaeobot Palynol* 90:339–360.
- Endress PK (1999) *Int J Plant Sci* 160:S3–S23.
- Cronk QCB (2001) *Nat Rev Genet* 2:607–619.
- Cronk QCB, Moller M (1997) *Trends Eco Evol* 12:85–86.
- Sargent RD (2004) *Proc R Soc London Ser B* 271:603–608.
- Stebbins GL (1974) *Flowering Plants: Evolution Above the Species Level* (Harvard Univ Press, Cambridge, MA).
- Donoghue MJ, Ree RH, Baum DA (1998) *Trends Plant Sci* 3:311–317.
- Luo D, Carpenter R, Vincent C, Copsey L, Coen E (1996) *Nature* 383:794–799.
- Luo D, Carpenter R, Copsey L, Vincent C, Clark J, Coen E (1999) *Cell* 99:367–376.
- Hileman LC, Kramer EM, Baum DA (2003) *Proc Natl Acad Sci USA* 100:12814–12819.
- Gübitz T, Caldwell A, Hudson A (2003) *Mol Biol Evol* 20:1537–1544.
- Feng X, Zhao Z, Tian Z, Xu S, Luo Y, Cai Z, Wang Y, Yang J, Wang Z, Wenig L, et al. (2006) *Proc Natl Acad Sci USA* 103:4970–4975.
- Citerne HL, Luo D, Pennington RT, Coen E, Cronk QCB (2003) *Plant Physiol* 131:1042–1053.
- Corley SB, Carpenter R, Copsey L, Coen E (2005) *Proc Natl Acad Sci USA* 102:5068–5073.
- Almeida J, Rocheta M, Galego L (1997) *Development (Cambridge, UK)* 124:1387–1392.
- Galego L, Almeida J (2002) *Genes Dev* 16:880–891.
- Costa MM, Fox S, Hanna AI, Baxter C, Coen E (2005) *Development (Cambridge, UK)* 132:5093–5101.
- Cubas P, Lauter N, Doebley J, Coen E (1999) *Plant J* 18:215–222.
- Doebley J, Stec A, Gustus C (1995) *Genetics* 141:333–346.
- Howarth DG, Donoghue MJ (2006) *Proc Natl Acad Sci USA* 103:9101–9106.
- Cubas P (2004) *BioEssays* 26:1175–1184.
- Cubas P, Coen E, Zapater JM (2001) *Curr Biol* 11:1050–1052.
- Cubas P, Vincent C, Coen E (1999) *Nature* 401:157–161.
- Endress PK (1992) *Int J Plant Sci* 153:S106–S122.
- Smyth DR, Bowman JL, Meyerowitz EM (1990) *Plant Cell* 2:755–767.
- Kosugi S, Ohashi Y (1997) *Plant Cell* 9:1607–1619.
- Lupas A, Van Dyke M, Stock J (1991) *Science* 252:1162–1164.
- Gaudin V, Lunness PA, Fobert PR, Towers M, Riou-Khamlich C, Murray JA, Coen E, Doonan JH (2000) *Plant Physiol* 122:1137–1148.
- Nath U, Crawford BC, Carpenter R, Coen E (2003) *Science* 299:1404–1407.
- Palatnik JF, Allen E, Wu X, Schommer C, Schwab R, Carrington JC, Weigel D (2003) *Nature* 425:257–263.
- Citerne HL, Pennington RT, Cronk QCB (2006) *Proc Natl Acad Sci USA* 103:12017–12020.
- Girurfa M, Dafni A, Neal PR (1999) *Int J Plant Sci* 160:S41–S50.
- Gómez JM, Perfectti F, Camacho JP (2006) *Am Nat* 168:531–545.
- Zachgo S, Silva Ede A, Motte P, Tröbner W, Saedler H, Schwarz-Sommer Z (1995) *Development (Cambridge, UK)* 121:2861–2875.
- Bey M, Stüber K, Fellenberg K, Schwarz-Sommer Z, Sommer H, Saedler H, Zachgo S (2004) *Plant Cell* 16:3197–3215.
- Zachgo S (2002) in *Molecular Plant Biology*, eds Gilmartin P, Bowler C (Oxford Univ Press, Oxford), pp 41–63.
- Clough SJ, Bent AF (1998) *Plant J* 16:735–743.